technical transactions

No. 2022/001

mechanics

sciendo

Optimisatin of a mobile device frame structure – practical aspects

Wiesław Jasiński
jasinski@witi.wroc.pl | https://orcid.org/0000-0002-1792-8724
Piotr Krysiak
krysiak@witi.wroc.pl | https://orcid.org/0000-0002-4760-5053
Cezary Pichlak
pichlak@witi.wroc.pl | https://orcid.org/0000-0002-1442-6796
Military Institute Of Engineering Technique, Wrocław
Krzysztof Ludian
k.ludian@hsw.pl | https://orcid.org/0000-0003-3209-3769
Huta Stalowa Wola

Scientific Editor: Jacek Pietraszek, Cracow University of Technology
Technical Editor: Aleksandra Urzędowska, Małgorzata Mazur, Cracow University of Technology Press
Language Verification: Timothy Churcher, Merlin Language Services
Typesetting: Anna Basista, Cracow University of Technology Press

Received: December 21, 2021
Accepted: February 2, 2022

Data Availability Statement: All relevant data are within the paper and its Supporting Information files.

Competing interests: The authors have declared that no competing interests exist.

Citation: Jasiński, W., Krysiak, P., Pichlak, C., Ludian, K. (2022). Numerical analysis of laser-welded flange pipe joints in lap and fillet configurations. *Technical Transactions*: *e2022001*. https://doi.org/10.37705/TechTrans/e2022001

Abstract

This paper presents a strength analysis of a steel container frame fastened to a Jelcz 8x8 chassis with four ISO 1161 corners. As part of the work, optimisation of the structure was performed using the numerical finite element method (FEM) and experimental tests with the use of strain gauges. The results of simulations and tests are summarised in appropriate tables and in the form of the distribution of stress contour lines using the Huber-Mises hypothesis.

Keywords: support frame, optimisation, strength calculations, strength tests

1. Introduction

In the present state of science and technology, computational methods have become a powerful tool and the ability to use them is indispensable for a modern engineer, constructor, technologist or scientist. The role of these methods is useful in the observation and description of phenomena, processes and materials. There is also a need to research new phenomena resulting from changing environmental conditions, e.g. working in a different atmosphere or researching new materials. All these activities require a significant number of precise validation measurements (Dietrich, 1986).

The hypotheses and mathematical models put forward based on observations must be verified by subsequent experimental studies, often on real models. The verification of hypotheses or theories by numerical experiments must also be based on constitutive relationships, boundary and initial conditions, which can only be established on the basis of experimental research. For complex systems, structures with complex geometry or those made of materials with complex properties, hybrid methods combining experimental and numerical research are effective. The obtained measurement results are processed and become the basis for calculations, which in turn, determine the next stage of the research.

The results of experimental tests are recognised evidence of the correctness of decisions made by the designer based on intuition, professional experience or simplified engineering calculations.

Most often, designers present two basic approaches to the issue:

a) The method of oversizing, i.e. excess of the material. This entails deliberate stiffening of the structure. This is, of course, associated with an increase in the cost of production, but in return, it significantly reduces the risk of failure and costly repairs needed during the operation of the device. This method is especially applicable for unit projects with a short implementation time.
b) Insufficient method, i.e. material minimisation. This consists of deliberately under-stiffening the structure. Such a procedure makes it possible to carry out relatively simple tests during production, allowing the sensible and optimal stiffening of the designed structure. Such tests consist of a trial loading of the structure and observation of critical places where additional reinforcements and struts or ribs are introduced. This method is especially applicable for unit projects, when there are workshop possibilities to perform the necessary tests.

Designing devices intended for repetitive (serial) production requires greater care. Measures to optimise the production costs, durability and energy efficiency of the product are indicated here. Strength calculations are common practice. With the development of design software, apart from traditional analytical methods, the finite element methods (FEM), the boundary element method MEB or the finite difference method MRS have also become increasingly important. In light of this, there is a need to verify the correctness of the results of the calculation methods. Various methods can be used to verify the results, for example, the FEM and the analytical method, but it is best to verify the results through experimental tests. With regard to the testing of the correctness of the structure's operation, i.e. the levels of stresses occurring in them, the most popular method is the measurement of deformations with the use of strain gauges.

Input data are the most important for the correct course of calculations. It is vital to specify the support points of the structure as well as the locations and values of loads. In most cases, the correct determination of loads, as well as the locations and types of bonds in supports, is not difficult. The only problem may be the size and complexity of the structure where the multitude of data significantly extends the calculation process, thus making it irrational. Similar issues were discussed in the works (Jabłońska-Krysiewicz, 2015; Wang, 2021; Abry et al., 2018; Turlier, 2014; Niemi et al., 2018; Fricke et al. 2006). These issues also apply to detachable – bolted and non-detachable – welded connections, which occur in these types of load-bearing structures.

https://doi.org/10.37705/TechTrans/e2022001

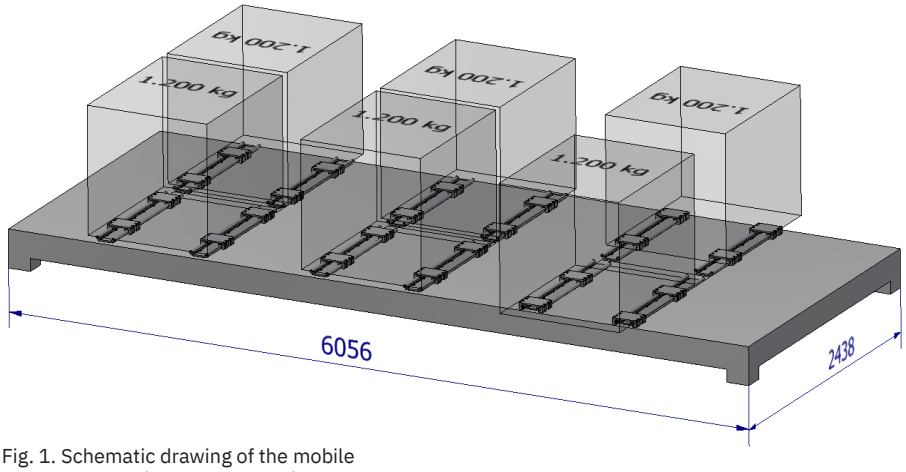

Fig. 1. Schematic drawing of the mobile platform frame (own elaboration)

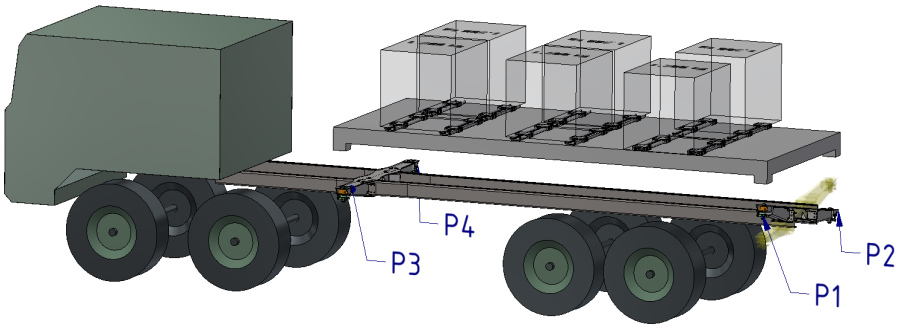

Fig. 2. Scheme of the mobile frame placed on a carrier vehicle, where: P1-P4 – points of reaction forces working on the frame corners (own elaboration)

This study presents a specific methodology that enables the avoidance of the problems presented above. Generally, this methodology is based on a simplification consisting of distinguishing individual functional systems and calculating them separately, taking into account the relations between them.

The work aimed to design a mobile platform frame (Fig. 1) intended for off-road trucks (Fig. 2) adapted to the container system (ISO 1161 corners). The frame is fastened to the vehicle frame and together they constitute the load-bearing structure. The load of the mobile frame is six containers with the possibility of transverse sliding on the rails. The shifting systems are equipped with electric drives. Each container weighs 1,200 kg.

2. Materials and methods

Autodesk Inventor Professional 2021 version 2021.3.3 was used to design the frame structure. The program contains the necessary mechanical standards and several useful calculation modules and wizards. For the purposes of this work, a steel profile library, a frame structure wizard, a shape generator (for initial frame shape optimisation) and frame structure analysis (for profile calculations) were used.

Autodesk Inventor Nastran version 2021.3.0.494 was used to perform mechanical calculations with the FEM. The method of linear analysis was used. A lower-order finite element mesh was determined with a size adapted to the structural elements used. All calculations were performed using the same grid so that the results were directly comparable.

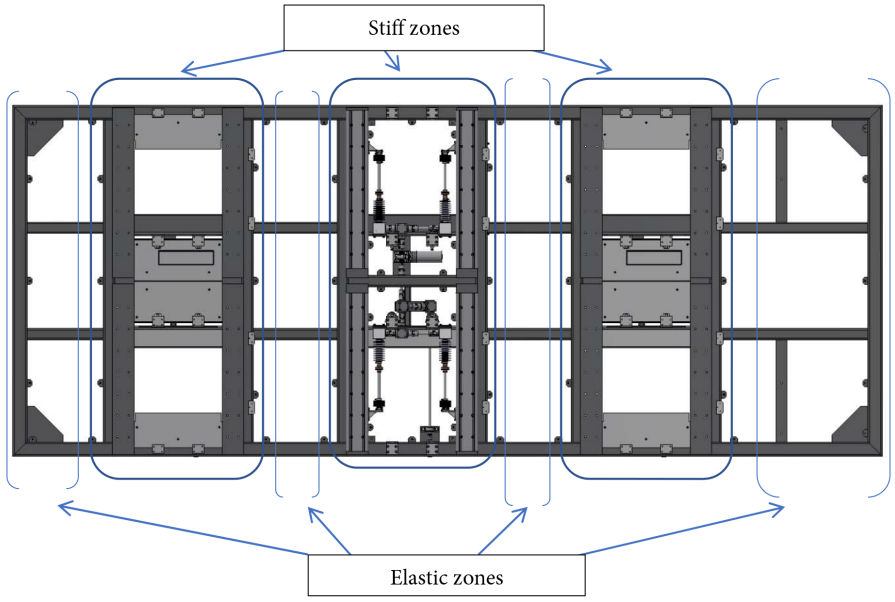

Fig. 3. Scheme of the section of the frame (own elaboration)

The basic assumptions about the frame are that the frame should contain rigid sections and flexible sections (Fig. 3). The rigid sections serve as the basis for lashing for six containers arranged in three two--container modules. The distance between modules should be minimal, but it should allow the containers to rotate freely around their vertical axes without collision. The containers for rotations should slide outwards on special rails from the longitudinal axis of the vehicle. It was assumed that the part of the platform from the side of P1 and P2 corners is longer to provide an additional loading area.

3. Research results and discussion

The aim of this study was to perform strength calculations of the load-bearing frame structure that functions together with the vehicle chassis, therefore their mutual interactions cannot be ignored. However, these interactions can be included in the basis for calculating the support frame of interest. These impacts were taken into account as motion forces (shape deviations) in the calculation basis. The course of the procedure is presented below.

The mobile platform should be resistant to twists of the vehicle support frame (supports P1 and P2 relative to to P3 and P4) due to the susceptibility of the drive system during off-road driving (Fig. 2). Thus, in the strength calculations, it is not enough to specify the weight load of the transported containers. The calculations should also take into account the stresses resulting from the elastic deformations of the frame occurring here.

3.1. Implementation of the frame design – optimization process

In the beginning, the optimisation of the frame shape (topographic analysis) was performed using the Inventor shape generator (Fig. 4), the operating algorithm of which detects the volumes within which the stresses are transferred, and removes the remaining volumes. it will remove the material.

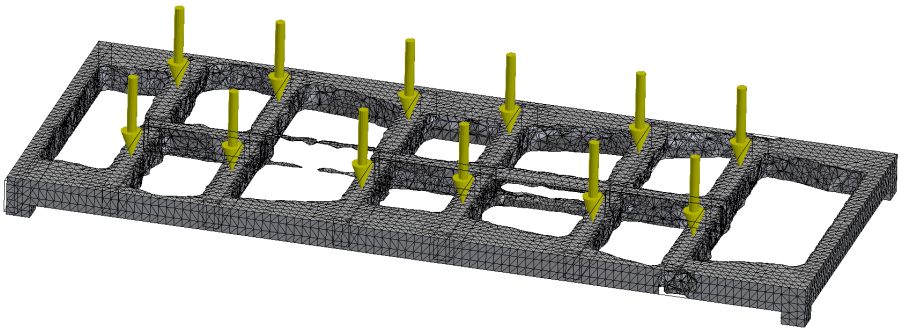

Fig. 4. The first step of the frame optimisation (own elaboration)

For the second run of the generator (Fig. 5), the arrangement of the profiles constituting the frame was marked, which results from the location of the designed mechanisms and accessories.

Figure 5 shows that the stringers need to be strengthened (especially in the middle of the frame) because at these points, the program indicates the need for more construction material; it is obvious that the longest beam subjected to bending loads should be reinforced. It is only necessary to specify what profile to use to strengthen the stringers. For this purpose, the analysis of two variants of the stringer reinforcement was performed:

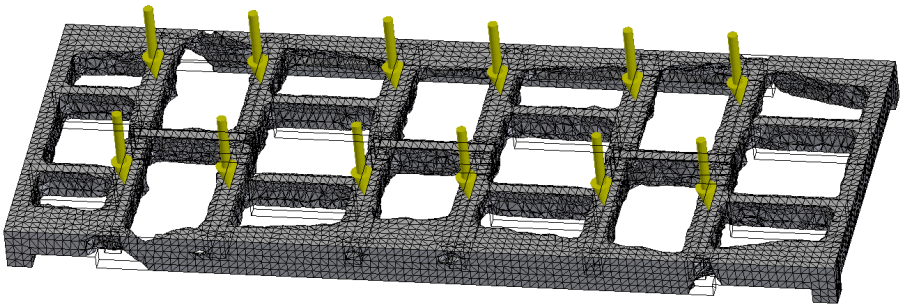

Fig. 5. The second step of the frame optimisation (own elaboration)

a) Profile 100 x 200 x 6 + Profile100 x 100 x 6
b) Profile 100 x 200 x 6 + Channel 100

The strength analysis for the specified stringer cross-sections was performed using the Inventor beam wizard. After performing the calculations using the Huber-Mises hypothesis, the following values of stresses and displacements were obtained.

Table 1. Summary of the calculated values

Cross section	Maximum stress [MPa]	Maximum deflexion [mm]
beam 100 x 200 x 6 + 100 x 100 x 6	101.7	11.4
beam 100 x 200 x 6 + C100	106.4	14.2

The preliminary results of the performed calculations can be considered comparable. However, the above analysis is incomplete as it concerns only

https://doi.org/10.37705/TechTrans/e2022001

the longitudinal beams (the most important for load transfer). There are also crossbeams in the frame, which also carry loads. Therefore, it is necessary to calculate the strength of the entire frame. Calculations should be made for both variants of the stringers' reinforcement.

It is not sufficient to perform strength calculations for a loaded frame set on four supports. Their forced displacements at the corners defined as P1 and P2 must also be taken into account (Fig. 2). The supports are elements of the frame of the carrying vehicle. During off-road driving, as a result of twisting of the vehicle frame, support P1 deflects upwards and support P2 downwards by the same amount (also vice versa). The magnitude of the deflection will be counterbalanced by the reaction forces induced on the frame in question. The analysis of the dependence between vertical wheel displacement, spring force, torsion force of the vehicle frame and vertical displacement of the support is complex and difficult to perform.

This problem can be solved on the assumption that the deformed vehicle frame is in equilibrium with the deformed support frame. During the deflection of the supports, the reactions in the corners of the mobile frame are equivalent to the deformation forces of the vehicle support frame. It is possible to assume the value of support deviation for calculations and determine for them the occurring stresses and reaction forces in the supports. In this way, a complicated analysis of forces and displacements of the system can be avoided. Particularly, the difference in the reactions in the P1 and P2 supports determines the ability of the frame to overcome terrain unevenness. Naturally, a comparable situation occurs when considering the opposite pair of reactions in supports P3 and P4, depending upon which pair of supports are taken as the reference element. Here, P3 and P4 are assumed to be stationary, and P1 and P2 as susceptible to motion.

The above reasoning is at the core of the adopted methodology of simplifying technical calculations, limiting them to a selected functional mechanical system, thus avoiding the necessity of jointly calculating the entire complete mechanism.

In this paper, a series of calculations was performed for the forced deviations of the P1 and P2supports, obtaining the corresponding reactions and stresses in the structure. The maximum stress readings may be the result of a methodological peculiarity. Therefore, there are also two points for reading the stresses in the centre of the main beams (where they should be physically greatest – Fig. 6). The correct solution is such forcing of the deflection of the supports, in which the stresses are under the permissible values of elastic stresses (no plastic deformation), while the read off difference in the reactions on the P1 and P2 supports is a measure of the vehicle's resistance to overcoming unevenness (torsion of the vehicle frame).

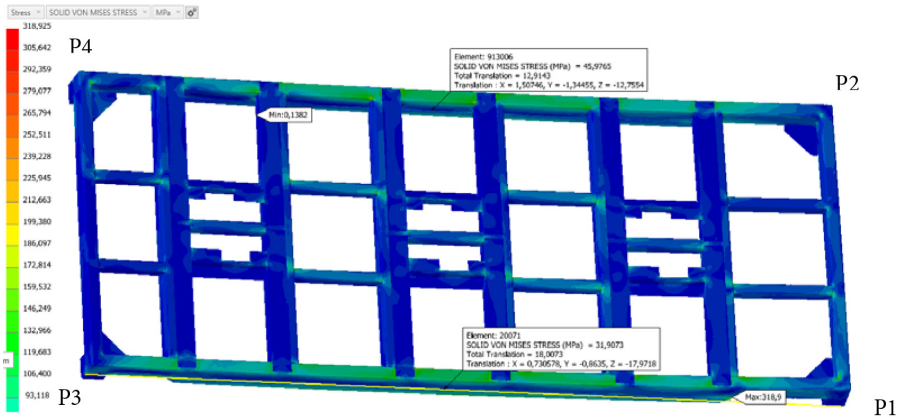

Fig. 6. Example simulation for the frame under displacement of 15 mm or -15 mm for P1 and P2, respectively (own elaboration)

The calculation results are presented in Table 2. An example of the obtained results is shown in Fig. 6, which illustrates the calculations recorded in Table 1, item 15.

Table 2 summarises the results of the FEM calculations using the Inventor Nastran software.

The calculations were made for two versions of the frame structure:

- Execution A – stringers reinforcement with C100 channel
- Execution B – stringers reinforcement with a 100x100x6 profile

Figure 7 compares the values of maximum stresses σ_{max} for both reinforcements. A linear increase in the stress is visible with the increase of the frame deformation force (the effect of the vehicle chassis). For the consistency

of calculations, a uniform FEM geometric mesh was adopted for each value of the supports' displacement. Under such conditions, the maximum stresses appear at the same places on the frame. It should be noted that the value of the maximum stress may not be reliable due to the emerging singularities, which is a feature of the FEM calculation methodology. For this reason, values exceeding the yield point of the material should not be taken into account (especially when they occur in unexpected places where there is complex and discontinuous geometry). Figure 7 shows the stress courses for both versions. These courses reveal no significant differences. It is interesting that for small displacement, the stresses for the reinforcement with the 100 x 100 profile are greater than for the C100 channel. This may be related to better frame flexibility with C100 reinforcement. An interesting point on the graph is that relating to displacement of 15 mm and stress of 320 MPa for which the graphs for both versions converge. This point symbolises the assumed elastic limit, above which the deformations are plastic (irreversible).

Table 2. Summary of calculation performed using FEM in the Inventor Nastran software

Type of reinforcement	Displacement		Registered forces				Max tension	Tension at mid–point		Deflexion
	P1 [mm]	P2 [mm]	P4 [N]	P3 [N]	P1 [N]	P2 [N]	σ_{max} [MPa]	σ_1 [MPa]	σ_2 [MPa]	
C100	0	0	22,705	22,582	20,989	20,925	181.3	105.4	104.1	12.8
	5	-5	25,827	19,458	24,276	18,635	221.8	108.6	100.4	–
	10	-10	28,973	16,314	28,642	16,075	265.2	111.8	97.0	–
	15	-15	32,108	13,178	32,682	13,682	313.9	116.7	95.1	–
	20	-20	35,243	10,043	36,678	11,283	418.3	120.4	91.7	–
	25	-25	38,378	6,908	40,656	8,881	522.7	124.0	88.4	–
	30	-30	41,513	3,773	44,625	6,478	627.2	127.7	85.0	–
	40	-40	47,782	-2,497	52,550	1,670	836.1	135.1	78.4	–
	50	-50	54,051	-8,767	60,466	-3,139	1,045.0	142.5	71.9	–
	80	-80	72,859	-27,577	84,194	-17,569	1,672.0	165.0	53.8	–
	150	-150	116,743	-71,468	139,530	-51,245	3,134.0	213.7	28.5	–
100 x 100 prof.	0	0	22,717	22,709	20,996	21,047	244.0	38.4	34.3	11.7
	5	-5	26,075	19,353	19,996	14,360	259.6	40.7	32.4	–
	10	-10	29,438	15,989	21,782	9,323	288.9	43.3	31.6	–
	15	-15	32,801	12,627	23,087	4,104	318.9	46.0	32.0	–
	20	-20	36,164	9,264	24,226	-1,226	411.8	48.8	33.1	–
	25	-25	39,527	5,903	25,293	-6,608	517.4	51.8	35.3	–
	30	-30	42,889	2,541	26,321	-12,017	623.1	55.0	38.1	–
	40	-40	49,614	-4,182	28,321	-22,878	834.4	61.8	45.5	–
	50	-50	56,339	-10,905	30,280	-33,767	1,046.0	69.2	54.3	–
	80	-80	76,512	-31,075	36,071	-66,501	1,680.0	92.9	84.5	–
	150	-150	123,584	-78,138	49,441	-142,983	3,160.0	161.5	151.8	–

Figure 8 compares the stress values σ_1 in the centre of the frame for both reinforcements. It was assumed that the stress was read in the centre of the frame from the bottom of the loaded stringer, where the most intuitive overloads

https://doi.org/10.37705/TechTrans/e2022001

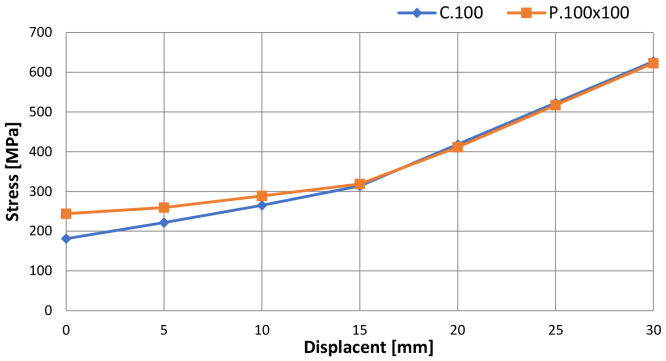

Fig. 7. Relationship between maximum tension (σmax) and displacement for both types of reinforcements (own elaboration)

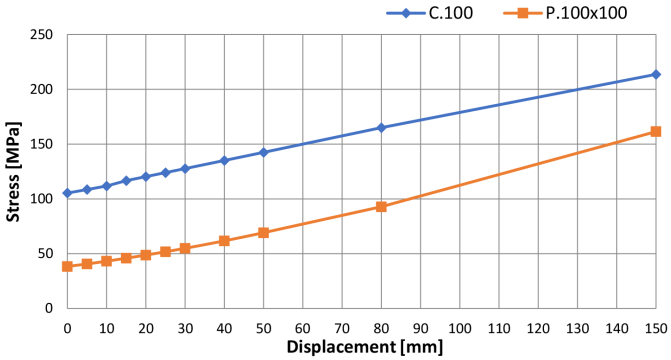

Fig. 8. Relationship between maximum tension (σmax) at the frame midpoint and displacement for both types of reinforcements (own elaboration)

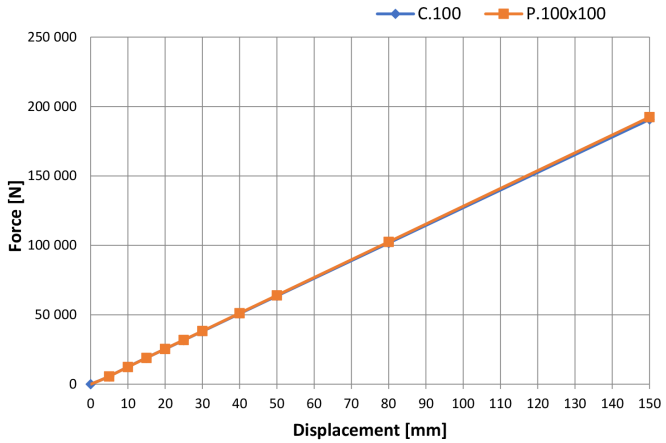

Fig. 9. Results of force difference for different reinforcements upon displacement (own elaboration)

occur. The stresses from Table 2 column σ_1 as larger because they reflect the stress on the more loaded stringer (the one that is lifted). This can be observed (confirmed) in the calculation results after the stresses marked as maximum (in singularity points) are rejected.

After a series of calculations, a linear increase in the stress σ_1 is visible with an increase in the frame force (the effect of the vehicle chassis). For the sake of consistency of calculations, a uniform geometric mesh was adopted for each value of the supports' displacement. Figure 8 shows the stress courses for both versions - the relationships are clearly linear. The obtained stresses do not exceed the maximum allowable elastic stresses, which for S235 steel are 235 MPa. The diagram shows that for the C100 channel reinforcement, they are significantly larger (although acceptable).

Table 3 shows the dependence of the calculated difference of the reaction forces P1-P2 in relation to the forced vertical displacement of the supports. This relationship is proportional – the greater the displacement of P1 and P2, the greater the ability to transmit torsional forces in the vehicle frame (road resistance). The comparison of the columns for P1 and P2 shows that both variants are functionally identical and fulfil the same role.

Table 3. Relationship between force difference and displacement

No.	Type of reinforcement		C100	100x100
	Displacement		Force difference	
	P1 [mm]	P2 [mm]	P1-P2 [N]	P1-P2 [N]
1	0	0	64	-51
2	5	-5	5,641	5,636
3	10	-10	12,567	12,459
4	15	-15	19,000	18,983
5	20	-20	25,395	25,452
6	25	-25	31,775	31,901
7	30	-30	38,147	38,338
8	40	-40	50,880	51,199
9	50	-50	63,605	64,047
10	80	-80	101,763	102,572
11	150	-150	190,775	192,424

The differences in the reactions on the supports shown in Table 3 and Fig. 9 illustrate the ability to transfer forces occurring during off-road driving (the vehicle frame is elastic). It can be seen that these forces are proportional to the applied displacement. Furthermore, for both versions (the C100 and the 100 x 100 one) they are practically identical. This does not answer the question which reinforcement type should be chosen.

Figure 7 shows that for the 100 x 100 profile reinforcement, the stresses σ_1 in the centre of the frame are lower by half than for the C100 reinforcement. This means that the use of 100x100 would be uneconomical given low-stress values. From the analysis of the maximum stress diagram σ_{max} (Fig. 7), it is possible to identify a better elasticity of the supporting frame (with containers), which may be of significant operational importance. The stresses exceeding the elastic limit (i.e. destructive) appear for both versions (C100 and 100 x 100) for the same values of the support forces (above ± 15 mm).

As a consequence of the performed calculations and evaluation of the results, it can be stated that:

- the structure has been designed correctly;
- it is more optimal to use reinforcement of the frame side members with C100 channels than with 100 x 100 profiles.

3.2. FEM calculations check – empirical tests

After the frame was made in metal, it was glued with strain gauges at selected points and loaded according to the required specifications. The aim was to verify the correctness of the results calculated using FEM and utilizing strain measurements.

The stress values calculated with FEM (see Fig. 10) are displayed in the points designated for the strain gauges.

Based on the calculated stress distribution, the points of strain gauge measurements in the frame were arranged. By comparing the stress values at these points, the correctness of the calculation method can be verified.

The designation of measuring points for stress tests (strain gauges) can be observed in Fig. 11.

Table 4 shows the comparison of the calculated results with the measured values. It can be concluded that at all measuring points, the calculated stress values are the same as the measured values. The deviations can be explained by the fact that the FEM stress reading point is not identical to the measuring surface of the strain gauge. In the area selected for measurement, the stresses are not uniform. In general, the calculated stresses are greater, which suggests that the calculations are reliable. It is important that the calculations are proportional to the values measured at the same points. The FEM calculation methodology can be considered to be correct.

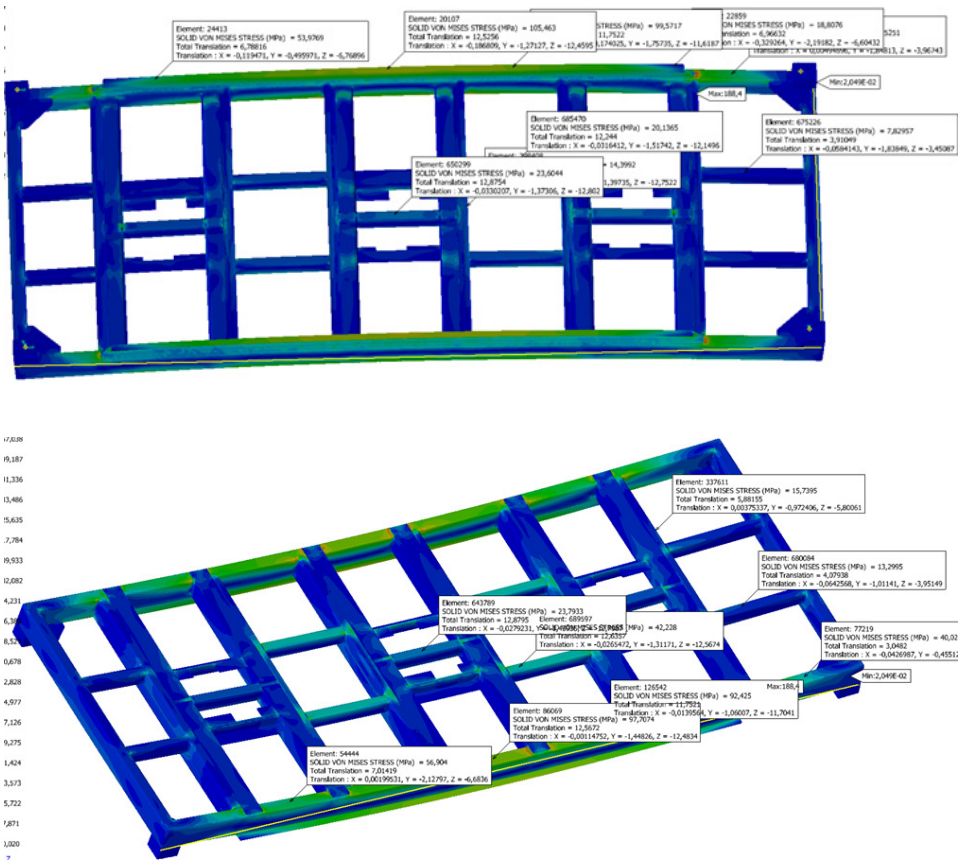

Fig. 10. Distribution of contour lines of stress values calculated using FEM (own elaboration)

https://doi.org/10.37705/TechTrans/e2022001

Fig. 11. Distribution of strain gauges 1–16 used to study the stress and, in red, the displacement gauge (*Przem*)

Table 4. Comparison of theoretical and empirical tension results

	Empirical results	Theoretical results from FEM	Tension difference [MPa]	Absolute deviation [%]
Gauge No.	σ_{max} [MPa]	σ_{zred} [MPa]		
1	-37.92	-40.0	2.1	-5.3%
2	35.73	58.5	22.8	39.0%
3	-9.34	-13.2	3.9	-29.5%
4	5.76	7.8	2.0	25.6%
5	-51.54	-92.4	40.9	-44.3%
6	60.54	99.5	39.0	39.2%
7	-27.29	-42.2	14.9	-35.3%
8	8.46	20.1	11.6	57.7%
9	-51.79	-97.7	45.9	-47.0%
10	62.29	105.4	43.1	40.9%
11	-26.02	-56.9	30.9	-54.3%
12	27.70	53.9	26.2	48.6%
13	-16.02	-23.7	7.7	-32.5%
14	12.46	23.6	11.1	47.0%
15	16.87	18.8	1.9	10.1%
16	19.76	14.3	-5.5	-38.5%
			average	37.2%

4. Conclusions

Performing comprehensive strength calculations brings undeniable benefits to design practice. This study shows that C100 C-profiles are a better solution for reinforcing the longitudinal members of a container frame than the seemingly stronger 100 x 100 profiles. As it turns out, the constructive intuition itself may turn out to be deceptive.

The study also presents a specific approach to defining input data for calculations, which significantly simplifies these calculations. It has been shown that individual components can be distinguished from the sum of mechanical systems. It is enough to define the forces and reactions at the connections of these systems.

References

Abry, J., Mittelhaeuser, C., Wolf, S., Turlier, D. (2018). Enhanced fatigue structural stress analysis of a heavy vehicle seam welded steel chassis frame: FEA model preparation, weld model description, fatigue stress calculation and correlation with 10 year operating experience. *Procedia Engineering*, Vol. 213, 539–548.

Dietrich, M. (1986). *Podstawy konstrukcji maszyn. Tom 1.* Warszawa: Państwowe Wydawnictwo Naukowe.

Fricke, W., Kahl, A., Paetzold, H., (2006). Fatigue Assessment of Root Cracking of Fillet Welds Subject to Throat Bending using the Structural Stress Approach. *Welding in the World*, Vol. 50, 64–74.

Jabłońska-Krysiewicz, A. (2015). Finite element modelling of the behaviour of steel end-plate connections. *Journal of Civil Engineering, Environment and Architecture*, Vol. 62, 173–184.

Niemi, E., Fricke, W., Maddox, S.J. (2008). *Structural Hot-Spot Stress Approach to Fatigue Analysis of Welded Components – Designer's Guide*. Second Edition. Springer Nature Singapore Pte Ltd.

Turlier, D., Klein, P., Bérard, F. (2014). FEA shell element model for enhanced structural stress analysis of seam welds. *Welding in the World*, Vol. 58, 511–528.

Wang, H., Zhang, B., Qian, H., Liu, J., An, B., Fan, F. (2021). Experimental and numerical studies of a new prefabricated steel frame joint without field--welding: Design and static performance. *Thin-Walled Structures*, Vol. 159.

https://doi.org/10.37705/TechTrans/e2022001